International Journal of Control, Automation, and Systems 22(9) (2024) 2882-2890
http://dx.doi.org/10.1007/s12555-023-0859-8
ISSN:1598-6446 eISSN:2005-4092
http://www.springer.com/12555

A Gripper Capable of Screw Fastening and Gripping With a Single Driving Source

Ji-Hun Meng, Inhwan Yoon, Sung-Jae Park, and Jae-Bok Song*

Abstract: As the range of applications of robots expanded, they began to be used for complex assemblies such as screw fastening and pin assembly. Most specialized screw fastening tools are sensitive to external influences and require additional instruments to prevent screw dislodgement when working in unstructured environments. To address this challenge, we propose a screw fastening gripper (SFG) capable of screw fastening and small pin gripping with a single power source. The proposed SFG is divided into a fastening part for screw fastening and a gripper for grasping, with power distributed via a magnetic gear. It is designed to temporarily separate the gripper and fastener using the magnetic gear's features, so it can be used to fasten screws of various lengths if necessary. Through gripping force measurements and screw fastening experiments, the proposed SFG showed sufficient performance in grasping and screw fastening.

Keywords: Assembly, gripper, magnetic gear, mechanism design, screw fastening.

1. INTRODUCTION

Collaborative robots are increasingly being used in complex operations such as assembly as well as simple parts transfer [1-3]. The assembly operations involve the assembly of small components such as screws and pins, and algorithms for this are constantly being developed. For stable peg assembly using a robot, the peg is grasped with a gripper and then a force control-based peg-in-hole strategy is used [4-7]. This strategy involves locating the target hole by interfering with the floor, so the gripper should be able to grip the peg tightly. The screw is a representative part used for assembly. In the case of automatic screw fastening devices [8,9] suited to previously developed robots, fast and stable screw fastening in a specific position is possible. However, when a screw is fastened in an unstructured environment, where the position of the assembly object is not fixed, it can be fastened using vision-based recognition task and peg-in-hole strategy, similar to the peg-in-hole process. In previously developed automatic screw fastening devices, the screw sometimes deviates when interference occurs in the screw located at the robot end.

The following two methods can be used to fasten screws using a robot in an unstructured environment. The first method involves using two robots equipped with a gripper and an electric fastener, similar to how a human works with both hands. However, using two robots for the simple task of screwing can be perceived as inefficient. The second method involves attaching a gripper and an electric fastening device to the end of the robot to execute the fastening work. However, because two devices are attached at the end, this method requires different power sources for the gripper and electric fastening device, increasing the price, and making it difficult to fasten screws at various angles in a narrow space. For example, a screwdriver of Onrobot [10] is 322 mm height and 114 mm width, and uses a spring-based holding mechanism at the tip of the tool to secure the screw position. This mechanism is not suitable for the peg-in-hole operation presented above as interference may cause the screw to deviate. To prevent this, an additional grasping tool can be used. For Schunk's compact parallel gripper [11], the stroke is 12 mm and the height is 88 mm and the width is 26 mm. When using both of these tools in parallel, a minimum height is 322 mm and a width of 140 mm would be required. Additionally, a screw tightening process becomes complicated because two tools must be controlled simultaneously.

This study proposes a screw fastening gripper (SFG) that allows both screw fastening and gripping with a single driving source to address this problem. The proposed system is significant in that two devices, which were previously operated independently by separate mechanisms such as a fastener for screw fastening and a gripper for

Manuscript received December 20, 2023; revised May 10, 2024 and July 5, 2024; accepted July 16, 2024. Recommended by Associate Editor Sangrok Jin under the direction of Senior Editor Jongeun Choi. This research was supported by the MOTIE under the Industrial Foundation Technology Development Program supervised by the KEIT (No. 20018188).

Ji-Hun Meng, Inhwan Yoon, Sung-Jae Park, and Jae-Bok Song are with the School of Mechanical Engineering, Korea University, 145, Anam-ro, Seongbuk-gu, Seoul 02841, Korea (e-mails: {men009, inhwan94, shurimia, jbsong}@korea.ac.kr).
* Corresponding author.

screw gripping, were merged into one system and executed two functions via a single driver. However, SFG is designed to leverage some of the strong rotational force required for screw fastening to drive the gripper, allowing screw fastening and gripping operations to be performed in parallel with a single motor. Because a single driving source is used, the system's size and price can be considerably decreased, while the user convenience is increased.

The rest of the paper is organized as follows: Section 2 describes the SFG's overall operating sequence and mechanism. In Section 3, the kinematics and statics of the SFG are analyzed. Section 4 examines the gripping force using a force/torque sensor, and the performance of the peg assembly and screwing using a robot. Finally, conclusions are drawn in Section 5.

2. SCREW FASTENING GRIPPER MECHANISM

2.1. Work sequence

Fig. 1 shows the screw fastening process using a SFG. After placing the gripper in position at the screw box where the screws are aligned (Fig. 1(a)), the screw is gripped with the gripper as shown in Fig. 1(b). Then the screw is moved to the screw hole where the fastening will be performed in Fig. 1(c). Finally, as shown in Fig. 1(d), the screw is fastened by rotating the fastening part while releasing the grip. At this point, because the screw's head is lowered in proportion to the rotation of the screw, the robot end must also be synchronized and lowered by the same distance.

As shown in Fig. 2, SFG can also be used for peg-in-hole assembly by gripping pegs instead of screws. First, after placing the gripper in the target hole in Fig. 2(a),

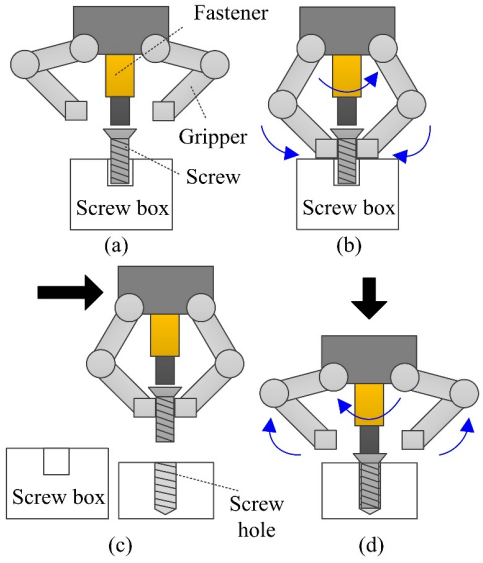

Fig. 1. Screw fastening process: (a) positioning, (b) grasping, (c) hole finding, and (d) fastening.

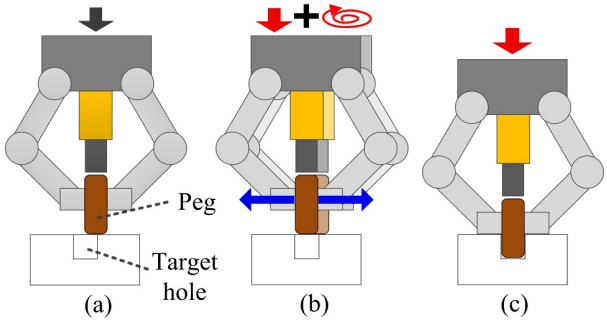

Fig. 2. Peg-in-hole assembly process: (a) positioning, (b) searching, and (c) inserting.

the robot applies force vertically and attempts to find the exact position of the hole by making a spiral motion near the hole in Fig. 2(b). Because of the vertical force, friction occurs between the peg and the surface, and a radial force is formed to push the gripper's tip. The proposed gripper is designed to withstand this force while maintaining the grip. Finally, as shown in Fig. 2(c), the robot lowers the gripper and completes the peg insertion.

2.2. Power transmission mechanism

The developed SFG is characterized by the fact that it uses both the rotational motion for screw fastening and the gripper's motion for gripping as a single driving source. Since the gripper inevitably has a mechanical range of motion, if the gripper's operation is completely restricted, the screw fastening process will also be stopped. Therefore, when fastening a long screw, the screw's rotation is also stopped when the gripper first reaches the limit of its range of motion. This can be solved using a mechanical solution such as a torque wrench which limits the transmitted torque, but the size of the system increases due to the complexity of the configuration. In addition, wear may occur due to mechanical friction, making it difficult to apply when limit situations occur repeatedly [12]. In this study, magnetic gear [13] is used in the power transmission mechanism to deal with this problem. The magnetic gear mechanism is shown in Fig. 3.

As shown in Fig. 3(a), the N and S poles of magnets are repeatedly attached to the gear surface to serve as gear teeth, and torque is transmitted using attractive and repulsive force between the poles. In this configuration, the gear ratio may be determined by the number of poles, and the transmission torque can be adjusted by changing the distance between the driving and driven gears. Furthermore, even if the driven gear is restricted by external factors and cannot rotate, as shown in Fig. 3(b), applying more than the transmission torque required to the driving gear causes a slip between the driving and the driven gears, allowing the driving gear to rotate. The magnetic gears used in the SFG are MGS3514 and MGC2112 provided by Gaon So-

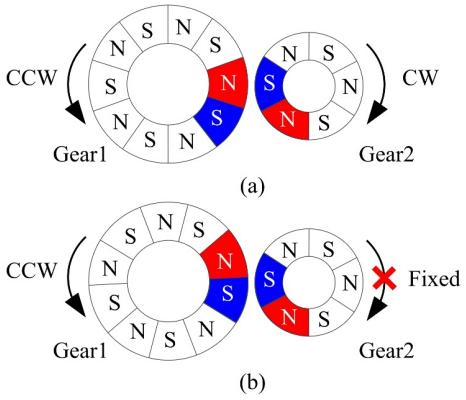

Fig. 3. Magnetic gear state of (a) gearing operation and (b) slipping operation.

Table 1. Torque transmission according to the air gap between magnetic gears.

Gear	Pole	Air gap (mm) & Torque (Nm)		
		0.5 mm	1.0 mm	1.5 mm
G_1	20	0.441	0.294	0.196
G_2	12	0.196	0.157	0.098

lution [14], and are referred to as G_1 and G_2 in this study. Unlike mechanical gears, magnetic gears use the attractive and repulsive forces between magnets, so it is difficult to calculate the transmitted torque using a simple formula. Table 1 shows the maximum torque that the gear can transmit depending on the air gap when using the two identical magnetic gears. When two different types of magnetic gears are combined for torque transmission, the delivered torque of each gear needs to be obtained experimentally, which is described in detail in Section 4.

Therefore, if the screw fastening part is connected to the driving gear and the gripper holding the screw is connected to the driven gear, the screw fastening and gripping process can be performed. When the gripper stops operating, the torque required for slip and the torque required for screwing the driving gear must be supplied at the same time. To this end, the transmission torque need to be set appropriately by adjusting the air gap between the magnetic gears.

2.3. SFG mechanism

The SFG mechanism proposed in this study is shown in Fig. 4. In the figure, G_1 and G_2 represent the driving and driven gears composed of magnets. The motor is connected to G_1 and is directly connected to the fastening part, while G_2 transmits a torque for the gripping operation. In the figure, V is the end of the fastener for screw fastening, P is the end of the gripper, and L_1, L_2, L_3, L_4, and L_5 are the links of the gripper. Link L_1 slides up and down through the rotation of the slide screw connected to

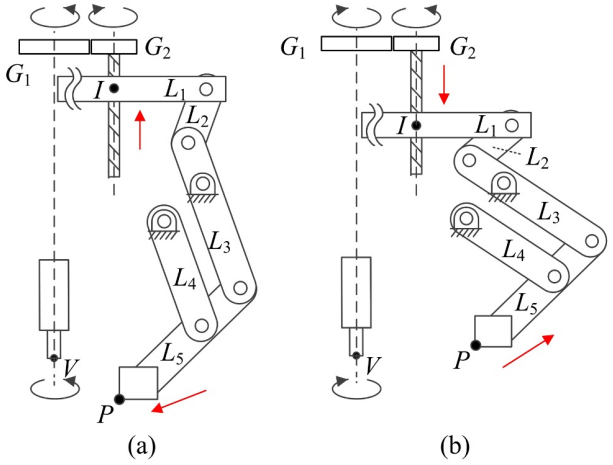

Fig. 4. Proposed SFG mechanism: (a) gripping motion and (b) screwing motion.

G_2. Because the gripper tip must move in parallel to grip pegs of various diameters, a parallel four-bar linkage is constructed between the gripper body and L_3, L_4, and L_5.

The gripping motion is shown in Fig. 4(a). When G_1 connected to the motor rotates counterclockwise, G_2 rotates clockwise, and L1 rises via a slide screw. Then the parallel four-bar linkage rotates via L_2, closing the gripper and performing a gripping operation. The screwing motion is shown in Fig. 4(b). Because the commonly used right-hand screws are tightened when rotating clockwise, G_1 rotates clockwise and G_2 rotates counterclockwise for fastening the screw. Since the gripper opens when the slide screw connected to G_2 rotates and L_1 attached to the nut descends, the gripper is designed to open automatically when the screw is tightened. G_2 stops rotating when L_1 reaches its operating limit and no longer descends. In this case, if G_1 is subjected to a torque exceeding the transmission torque between magnetic gears, G_1 continues to rotate while overcoming slip, allowing the screw fastening to continue. Therefore, since the fastening part can also be rotated, screw fastening of various lengths can be performed.

The design guidelines for SFG are as follows:

1) The gripper must open at a sufficiently fast speed so as not to interfere with screw fastening.
2) The effect of magnetic gear slip on screw fastening must be minimized.
3) The gripper end must provide sufficient gripping force for peg-in-hole tasks.

During the screw fastening process, SFG should not interfere with the fastening target. Therefore, the gripper must be opened through the rotation of driven gear while the driving gear directly connected to the fastening part rotates for screwing. According to ISO 724 [15], the pitch of each screw is approximately 1/6 of the diameter, and the

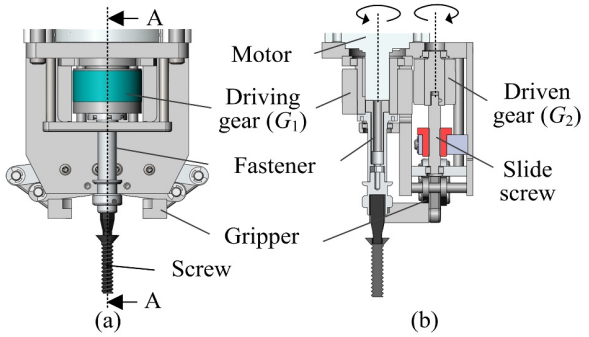

Fig. 5. Structure of SFG: (a) front view and (b) A-A cross-sectional view.

fastening depth of the screw for fastening is generally at least 1.5 times the screw diameter. Therefore, most screws require at least 9 rotations for tightening, during which time the gripper opening must be completed. Fig. 5 shows the structure of the designed SFG.

In this design, the gear ratio was set by adjusting the number of poles of the magnet gear to 5 : 3 to increase the rotation speed of the driven gear G_2. Therefore, while the driving gear G_1 rotates 9 times, G_2 rotates 15 times. Furthermore, the pitch of the slide screw connected to G_2 was selected to be 1 mm to reinforce the gripping force, and as a result, the slide nut moves 15 mm by 9 rotations of the driving gear.

3. KINEMATICS AND STATICS

In this section, the gripper operation is identified using kinematic and static analysis of the designed SFG, and the final gripping force is estimated by calculating the thrust of the slide screw. Through this, the material and dimensions are determined to ensure sufficient strength and durability when designing the gripper.

3.1. Kinematic analysis

Fig. 6 shows a vector-loop diagram of the gripper mechanism. In the figure, l_t is the relative position of the slide nut from the origin, l_1, l_2, l_3, l_4, l_5, and l_6 represent the link length, and θ_1 and θ_2 represent the link angle. The vector equations of the driving unit are as follows:

$$\overline{OI}+\overline{IJ}+\overline{JK}=\overline{OA}+\overline{AK}, \tag{1}$$

$$\overline{OP}=\overline{OA}+\overline{AB}+\overline{BE}+\overline{EP}, \tag{2}$$

where $a=\angle CAO$ is constant, and the position $P(p_x, p_y)$ of the final gripper tip is determined by θ_2. Since θ_2 is dependent on l_t, forward kinematics is defined as the problem of finding (p_x, p_y) for a given l_t. The point V that is the end of the screw fastening part must satisfy $|v_y| > |p_y|$ to prevent the gripper tip from colliding with the part to which the screw is fastened.

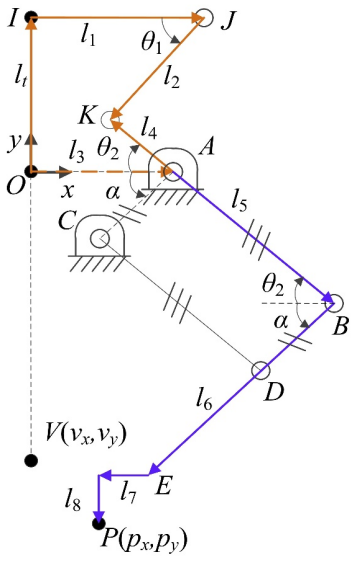

Fig. 6. Vector-loop diagram for gripper part.

Equation (1) can be expressed in terms of the parameters and variables in Fig. 6 as follows:

$$l_1-l_2\cos\theta_1=l_3-l_4\cos\theta_2, \tag{3}$$

$$l_t-l_2\sin\theta_1=l_4\sin\theta_2. \tag{4}$$

Elimination of θ_1 by combining (3) and (4) yields

$$k_{11}\cos\theta_2+k_{12}\sin\theta_2=k_{13}, \tag{5}$$

where $k_{11}=2(l_1-l_3)l_4$, $k_{12}=-2l_tl_4$, $k_{13}=l_2^2-l_4^2-l_t^2$. If $t_1=\tan(\theta_2/2)$ is defined, then (5) can be rearranged for t_1 as follows:

$$(k_{11}+k_{13}){t_1}^2-2k_{12}t_1+(k_{13}-k_{11})=0. \tag{6}$$

The above equation can be solve for θ_2 as follows:

$$\theta_2=2\tan^{-1}\left(\frac{k_{12}\pm\sqrt{{k_{12}}^2+{k_{11}}^2-{k_{13}}^2}}{k_{11}+k_{13}}\right). \tag{7}$$

Next, (2) can be expressed in terms of the parameters and variables in Fig. 6 as follows:

$$p_x=l_3+l_5\cos\theta_2-l_6\cos\alpha-l_7, \tag{8}$$

$$p_y=-l_5\sin\theta_2-l_6\sin\alpha-l_8. \tag{9}$$

Finally, (p_x, p_y) can be obtained as a function of l_t by substituting (7) into (8) and (9). The dimensions of SFG given in this study are shown in Table 2.

The length l_t, which represents the distance from O to the point I, by the linear drive of the slide screw is given by

$$l_t=l_{t,\max}-GP_s/R, \tag{10}$$

Table 2. Dimensions of SFG (α in deg and others in mm).

Parameters	l_1	l_2	l_3	l_4	l_5
Value	22	15	21.2	8	25
Parameters	l_6	l_7	l_8	v_y	α
Value	35	4	8	−36.4	36.8

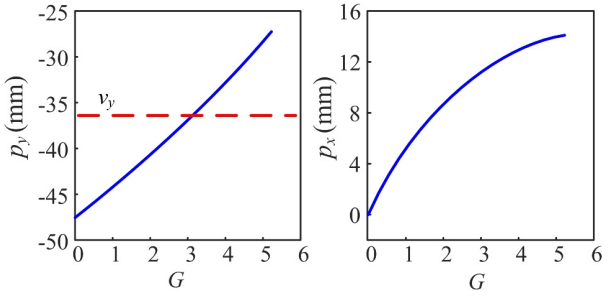

Fig. 7. Position of gripper tip according to the number of rotations of the driving gear.

where $l_{t,max}$ is the distance to I when the gripper is completely closed, G is the number of rotations of the driving gear, R is the reduction ratio of 5 : 3, and P_s is the pitch of the slide screw. In this study, $l_{t,max} = 21.6$ mm, and $P_s = 1$ mm. Therefore, (7), (8), (9), and (10) can be used to calculate the position $P(p_x, p_y)$ of the gripper tip as a function of G.

As mentioned above, screws generally require at least 9 rotations for tightening. A graph of p_x and p_y with G is shown in Fig. 7. After 3 rotations of the driving gear, the condition of $|v_y| > |p_y|$ is met, so the gripper can be opened at a sufficiently high speed, which is the first requirement given in Subsection 2.3.

3.2. Static force analysis

In this section, a static force analysis [16] of the gripper mechanism was performed to demonstrate that the gripper mechanism can generate a sufficient gripping force for the peg-in-hole task. Fig. 8 shows the free-body diagram (FBD) of the gripper mechanism. In the FBD of the link PDB, the reaction forces f_{54}, f_{53x}, and f_{53y} can be obtained by

$$\sum F_x = f_e - f_{54}\cos\theta_2 + f_{53x} = 0, \tag{11}$$

$$\sum F_y = f_{54}\sin\theta_2 + f_{53y} = 0, \tag{12}$$

$$\sum T_D = l_6 f_e \sin\alpha - l_{61} f_{54}\sin(\theta_2+\alpha) = 0, \tag{13}$$

$$f_{53x} = f_e\left(\frac{l_6\sin\alpha\cos\theta_2}{l_{61}\sin(\theta_2+\alpha)} - 1\right), \tag{14}$$

$$f_{53y} = -f_e\frac{l_6\sin\alpha\sin\theta_2}{l_{61}\sin(\theta_2+\alpha)}. \tag{15}$$

In the FBD of the link IJ, the reaction forces f_{1y} and f_{12} are given by

$$\sum F_y' = f_{1y} - f_{12}\sin\theta_1 = 0, \tag{16}$$

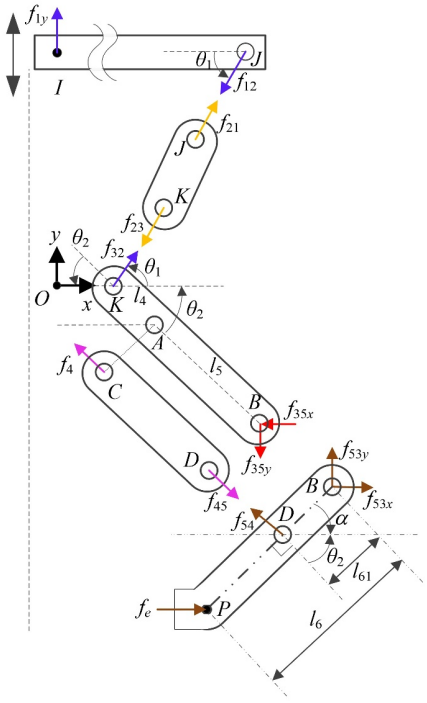

Fig. 8. Free-body diagram of SFG.

$$f_{12} = f_{1y}/\sin\theta_1. \tag{17}$$

In the FBD of the link JK, the reaction forces f_{21} and f_{23} are given by

$$\sum F = f_{21} + f_{23} = 0. \tag{18}$$

Since $f_{32} = -f_{23} = f_{21} = -f_{12}$, $f_{35x} = -f_{53x}$, $f_{35y} = -f_{53y}$ in the FBD, the reaction forces f_{32}, f_{35x}, and f_{35y} of the link KAB are described by

$$\begin{aligned}\sum T_A &= l_4 f_{12}\sin(\theta_1+\theta_2) + l_5 f_{53y}\cos\theta_2 \\ &\quad + l_5 f_{53x}\sin\theta_2 \\ &= 0.\end{aligned} \tag{19}$$

Substituting (14), (15), (18) into (19) yields

$$f_e = \frac{l_4\sin(\theta_1+\theta_2)}{l_5\sin\theta_1\sin\theta_2} f_{1y}. \tag{20}$$

As shown in (20), it is necessary to calculate the thrust of the slide screw f_{1y} to obtain f_e. In general, the efficiency η of changing the torque applied to the slide screw to the thrust is given by

$$\eta = \frac{1-\mu\tan\beta}{1+\mu/\tan\beta}, \tag{21}$$

where b is the lead angle of the thread and m is the coefficient of friction. Since the effective radius of the slide screw is 2.8 mm and the pitch is 1 mm, b is approximately 3.25°. Since the slide screw and nut are made of stainless

steel and brass, respectively, and no lubricant is used, m is assumed to be 0.5 [17]. Therefore, the efficiency h is calculated as 9.74%. The thrust of the slide screw is obtained from the transmission torque of the driven gear as follows:

$$f_{1y} = 2\pi\eta T_g / P_s, \tag{22}$$

where T_g is the transmission torque of the driven gear, and P_s is the pitch of the slide screw. Therefore, $f_{1y} = 96$ N since $T_g = 0.157$ Nm and $P_s = 1$ mm. By substituting this into (20), the gripping force according to the gripper motion can be estimated. The results will be discussed further in Section 4.

4. EXPERIMENTS AND RESULTS

In this section, the first experiment was conducted to measure the accurate transmission torque of G_1 and G_2. Two experiments were then conducted using the SFG manufactured as shown in Fig. 9 to check whether the design guidelines presented in Subsection 2.3 were satisfied. Maxon's EC 60 flat motor with a torque constant of 53 mNm/A and a current efficiency of 85% was used for the experiment. A GP 52 planetary gear [18] with a 26 : 1 reduction ratio and the gear efficiency of 83% was also installed to secure torque for screw fastening. The final size of SFG, including the motor and driver, is 230 mm height and 90 mm width.

4.1. Experiments on magnetic gears

If two different magnetic gears are combined together, the transmission torques shown in Table 1 may not be fully generated. Therefore, some experiments shown in Fig. 10 were conducted to accurately measure the transmission torque of the magnetic gears used in the SFG. The experiments were conducted by applying a torque to the magnetic gear connected with a handle while fixing the relative position with the other gear. As shown in Fig. 10(a), G_1 was connected to a commercial force torque sensor (FTS) [19], G_2 was rotated by a handle, and the maximum torque generated by G_1 was measured. Next, the same experiment was conducted after changing the roles of G_1 and

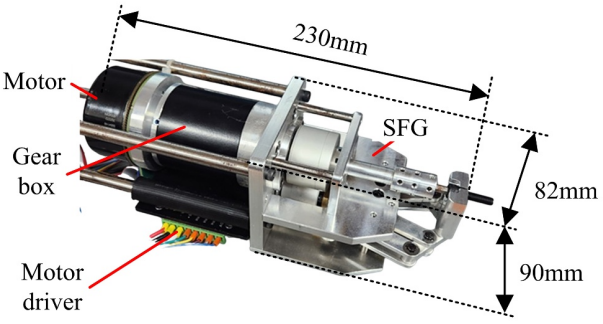

Fig. 9. Photo of the proposed SFG.

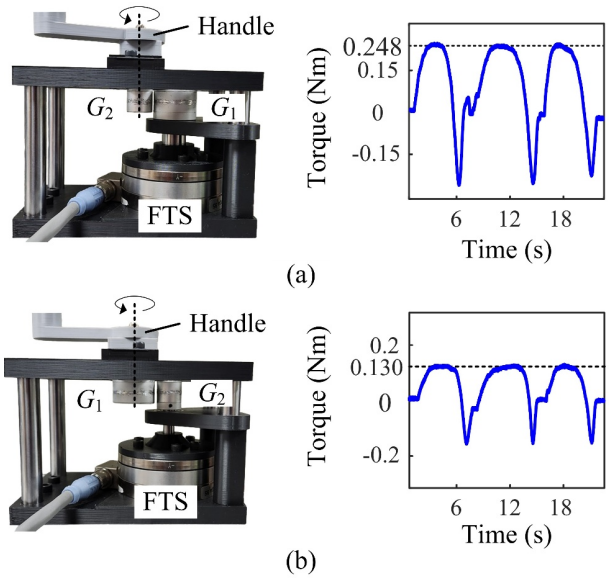

Fig. 10. Maximum tramsmission torque measurements of (a) G_1 and (b) G_2.

G_2, as shown in Fig. 10(b). In both experiments, the angle at which the magnetic gear was rotated when measuring torque was 1 pole pair, which is 36° and 60° for G_1 and G_2, respectively. To minimize the effects of vibration, the handle was rotated at a slow speed over approximately 5 seconds, and each test was repeated three times. The magnetic gears mounted in the SFG has an air gap of 1 mm.

As a result of the experiment, the average maximum transmission torque measured was 0.248 Nm for G_1 and 0.130 Nm for G_2. This is about 83% of the torque of 0.294 Nm and 0.157 Nm in Table 1. The change in maximum transmitted torque appears to be caused by changes in the attractive and repulsive forces between magnets due to differences in the number and size of poles of the magnetic gears.

4.2. Experiments on screw fastening

As mentioned before, slip between the two magnetic gears occurs at the limit of the range of motion, thus generating a repulsive force during the rotation of the fastening part. Therefore, this interference was minimized by adjusting the gap between the magnetic gears. In this experiment in which the M5 screw was fastened using the SFG attached to the robot as shown in Fig. 11, the repulsive force due to slip was indirectly obtained by estimating the motor output torque from the measured motor current. In Fig. 11(d) a low-pass filter with a cutoff frequency of 25 Hz was applied.

As shown in Fig. 11(a), the average current supplied to the motor during the process of rotating the screw while opening the gripper at the beginning of fastening was 2.4 A. At this point, magnetic gear slip did not occur, so only

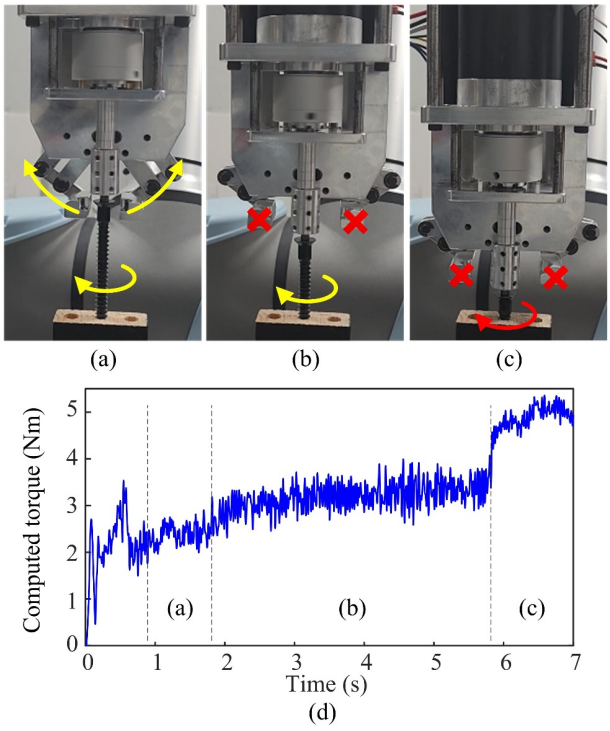

Fig. 11. Three stages of SFG operation of (a) screw rotation with gripper opening, (b) slipping operation, (c) screw fastening, and (d) computed torques estimated in three stages.

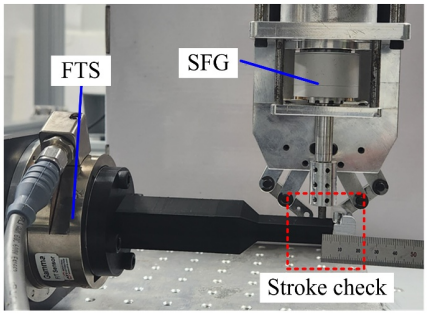

Fig. 12. Measurements of fingertip force.

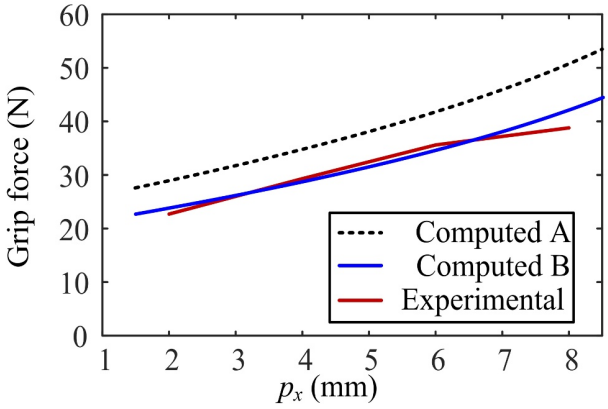

Fig. 13. Result of gripping force.

the current required for screw rotation was used. As shown in Fig. 11(b), the gripper reached its motion limit in the middle of fastening, causing the magnetic gears to slip, and the average current rose to 3.0 A when the screw was rotated.

Therefore, the average current difference due to slip was 0.6 A, and the average torque required for slip generation was estimated to be 0.58 Nm based on the reduction ratio and efficiency. The indirectly measured torque loss was 0.33 Nm higher than the maximum transmitted torque of G_1 measured in the experiment of Fig. 10(a). It is presumed that this error is due to the change in friction according to the screw fastening length and the occurrence of torque offset compared to the motor current due to friction inside the gearbox. As shown in Fig. 11(c), the average current used for screwing was 5 A, so the output torque during fastening was calculated to be 4.8 Nm, indicating that 4.2 Nm was used for screwing excluding 0.58 Nm required for slip. Therefore, it was confirmed that there were no problems with grasping and fastening the screw using the proposed SFG.

4.3. Experiments on gripping force

An experiment was performed as shown in Fig. 12 to examine the gripping force of SFG described in Subsection 3.2. Because SFG is designed to grasp small pegs such as pins or screws, the gripping force was measured when the gripper stroke was 4, 8, 12, and 16 mm, respectively, and the position p_x of the gripper tip was 2, 4, 6, and 8 mm, respectively. The experiment was performed by using a FTS to measure the maximum force applied to one gripper tip.

The gripping force for each location can be calculated by substituting the thrust of the slide screw calculated in Subsection 3.2 into (22). In the same way, the gripping force for each tip position can be calculated using the maximum transmission torque of G_2 measured in the experiment in Fig. 10(b).

Two computed gripping force and the measured data are compared as shown in Fig. 13. The actual gripping force was approximately 81% of the computed A value based on Table 1, and almost same with computed B value basd on Fig. 10(b).

An actual assembly task using an IKEA wooden chair was performed using the manufactured SFG. The SFG grasped a wooden pin with a diameter of 8 mm and inserted it into the hole using the peg-in-hole strategy.

Fig. 14(a) shows the peg-in-hole strategy applied to pin assembly using SFG, and Fig. 14(b) shows the result of measuring the radial force generated by friction, using a FTS attachted at the end of the robot. As shown in Fig. 14(b). the maximum radial force exerted on the pin in the

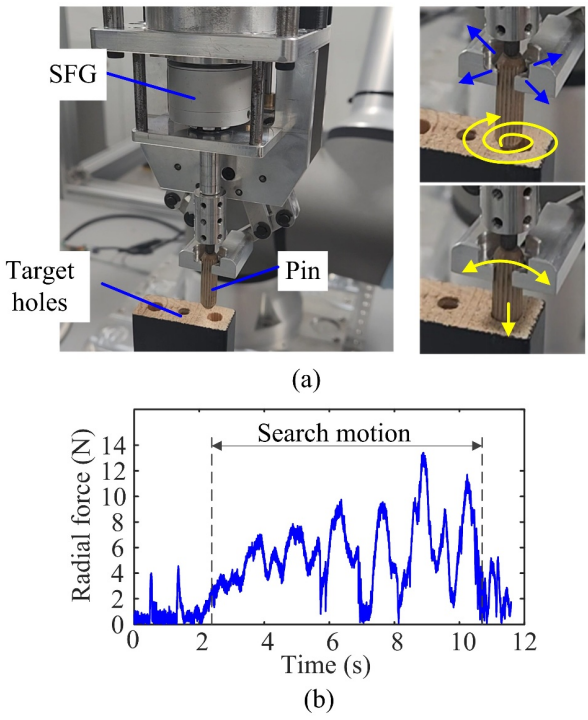

Fig. 14. Assembly experiments using (a) peg-in hole strategy and (b) axial force measurement using a force/torque sensor.

pin assembly was 14 N. To grasp a pin with a diameter of 8 mm, the tip position px of the SFG must be 4 mm. The gipping force measured at that position is 29 N in Fig. 12, confirming that sufficient gripping force can be provided, which is one of the design guidelines specified in Subsection 2.3.

5. CONCLUSION

Most screw fastening devices have weak holding forces, making screw fastening difficult in an unconstructed environment. This can be solved by using an additional small gripping tool, but the problem is that the system becomes larger and its control becomes more complicated. The SFG proposed in this study was designed as a mechanism capable of gripping and screwing in parallel while using a single driving source. Based on the kinematic and static analysis of the gripper mechanism, and experiments on screw fastening and gripping force, the following conclusions are drawn.

1) SFG was designed to open the gripper at a speed high enough to prevent interference between the gripper tip and the fastening object during screw fastening.
2) The torque loss of the fastening part caused by the magnetic gear slip from the time the gripper reaches the motion limit was measured 0.248 Nm, which is only 7% of fastening torque, so there is no problem for screw fastening.
3) The SFG mechanism can provide more than 20 N gripping force, which is sufficient to use the peg-in-hole strategy.

Therefore, torque loss during screw fastening was minimized, and sufficient grasping force could be provided through an appropriate air gap between magnetic gears. In addition, by implementing two operations through a single driving source, the entire system for screw fastening was simplified and reduced in size.

CONFLICT OF INTEREST

The authors declare that there is no competing financial interest or personal relationship that could have appeared to influence the work reported in this paper.

REFERENCES

[1] F. Suárez-Ruiz, X. Zhou, and Q.-C. Pham, "Can robots assemble an IKEA chair?" *Science Robotics*, vol. 3, no. 17, pp. 421-426, 2018.

[2] S. Park, H. Lee, S. Kim, J. Baek, K. Jang, H. C. Kim, M. Kim, and J. Park, "Robotic furniture assembly: Task abstraction, motion planning, and control," *Intelligent Service Robotics*, vol. 15, pp. 441-457, 2022.

[3] Y. Jiang, Z. Huang, B. Yang, and W. Yang, "A review of robotic assembly strategies for the full operation procedure: Planning, execution and evaluation," *Robotics and Computer-Integrated Manufacturing*, vol. 78, 2022.

[4] H. Park, J. Park, D.-H. Lee, J.-H. Park, and J.-H. Bae, "Compliant peg-in-hole assembly using partial spiral force trajectory with tilted peg posture," *IEEE Robotics and Automation Letters*, vol. 5, no. 3, pp. 4447-4454, 2020.

[5] I. F. Jasim, P. W. Plapper, and H. Voos, "Position identification in force-guided robotic peg-in-hole assembly tasks," *Procedia CIRP*, vol. 23, pp. 217-222, 2014.

[6] D.-H. Lee, M.-S. Choi, H. Park, G.-R. Jang, J.-H. Park, and J.-H. Bae, "Peg-in-hole assembly with dual-arm robot and dexterous robot hands," *IEEE Robotics and Automation Letters*, vol. 7, no. 4, pp. 8566-8573, 2022.

[7] H. Kang, Y. Zang, X. Wang, and Y. Chen, "Uncertainty-driven spiral trajectory for robotic peg-in-hole assembly," *IEEE Robotics and Automation Letters*, vol. 7, no. 3, pp. 6661-6668, 2022.

[8] D. Kim, "Automatic screw tightening machine," Korean Patent 1023416180000, December 21, 2021.

[9] SETech. Robot attachment NUT RUNNER: http://www.setech.co.kr/bbs/board.php?bo_table=eng2_2&wr_id=16.

[10] Onrobot, Multifunctional robot screwdriver with screw feeder: https://onrobot.com/ko/jepum/onrobot-screwdriver.

[11] SCHUNK, Gripper for small components: EGP 40-N-S-B: https://schunk.com/us/en/gripping-systems/parallel-gripper/egp/egp-40-n-s-b/p/000000000000310942.

[12] Tatsuya Amami, "TORQUE WRENCH," U.S. Patent US006742418B2, June 1, 2004.

[13] P. M. Tlali, R. Wang, and S. Gerber, "Magnetic gear technologies: A review," *Proc. of 2014 International Conference on Electrical Machines (ICEM)*, pp. 544-550, 2014.

[14] Gaon Solution, MAGNET GEAR: http://www.e-gaon.co.kr/gb/bbs/board.php?bo_table=en_product&wr_id=12&sca=10#!.

[15] International standard, ISO 724, "ISO general purpose metric screw threads-Basic dimensions," pp. 2-3, 2023.

[16] R. L. Norton, *Design of Machinery: An Introduction to the Synthesis and Analysis of Mechanisms and Machines*, McGraw-Hill, Inc. pp. 531-538, 2008.

[17] Engineers Edge, Coefficient of Friction Equation and Table Chart, Available online: https://www.engineersedge.com/coeffients_of_friction.htm.

[18] Maxon, EC 60 flat motor, GP 52 planetary gear: https://www.maxongroup.co.kr/maxon/view/content/index.

[19] ATI, F/T Sensor: gamma: https://www.ati-ia.com/products/ft/ft_models.aspx?id=gamma.

Ji-Hun Meng received his B.S. degree in mechanical engineering from Korea University in Seoul, Korea, in 2019. He is currently a Ph.D. candidate in mechanical engineering at Korea University. His research interests include manipulator design, gripper design, and collaborative robot arms.

Inhwan Yoon received his B.S. degree in mechanical engineering from Sogang University in Seoul, Korea, in 2019. He is currently a Ph.D. candidate in mechatronics at Korea University. His research interests include manipulator control, robotic assembly, and AI-based robot applications.

Sung-Jae Park received his B.S. degree in mechanical engineering from Korea University in Seoul, Korea, in 2019. He is currently a Ph.D. candidate in the mechanical engineering at Korea University. His research interests include gripper design and tool changer design.

Jae-Bok Song received his B.S. and M.S. degrees in mechanical engineering from Seoul National University in Seoul, Korea, in 1983 and 1985, respectively. He received his Ph.D. degree in mechanical engineering from M.I.T. in 1992. He is a professor in the Department of Mechanical Engineering in Korea University since 1993. His research interests include robot design and control, and AI-based robot applications. He is a senior member of IEEE.